



# Bilateral Symmetry Detection on the Basis of Scale Invariant Feature Transform

Habib Akbar<sup>1</sup>, Khizar Hayat<sup>1,2\*</sup>, Nuhman ul Haq<sup>1</sup>, Usama Ijaz Bajwa<sup>1</sup>

<sup>1</sup> COMSATS Institute of Information Technology, Abbottabad, Pakistan, <sup>2</sup> College of Arts and Sciences, University of Nizwa, Nizwa, Sultanate of Oman

## Abstract

The automatic detection of bilateral symmetry is a challenging task in computer vision and pattern recognition. This paper presents an approach for the detection of bilateral symmetry in digital single object images. Our method relies on the extraction of Scale Invariant Feature Transform (SIFT) based feature points, which serves as the basis for the ascertainment of the centroid of the object; the latter being the origin under the Cartesian coordinate system to be converted to the polar coordinate system in order to facilitate the selection symmetric coordinate pairs. This is followed by comparing the gradient magnitude and orientation of the corresponding points to evaluate the amount of symmetry exhibited by each pair of points. The experimental results show that our approach draw the symmetry line accurately, provided that the observed centroid point is true.

**Citation:** Akbar H, Hayat K, Haq Nu, Bajwa UI (2014) Bilateral Symmetry Detection on the Basis of Scale Invariant Feature Transform. PLoS ONE 9(8): e103561. doi:10.1371/journal.pone.0103561

**Editor:** Francesco Pappalardo, University of Catania, Italy

**Received:** January 10, 2014; **Accepted:** July 2, 2014; **Published:** August 21, 2014

**Copyright:** © 2014 Akbar et al. This is an open-access article distributed under the terms of the Creative Commons Attribution License, which permits unrestricted use, distribution, and reproduction in any medium, provided the original author and source are credited.

**Funding:** These authors have no support or funding to report.

**Competing Interests:** The authors have declared that no competing interests exist.

\* Email: khizarhayat@ciit.net.pk

## Introduction

Symmetry is an omnipotent phenomenon in real world objects, whether natural or artificial. An object is said to be symmetric, if there is a self-similarity or balance within the object, which can be proved according to the rules of a formal system, i.e. by geometry. Basically there are four types of symmetries in 2D Euclidean geometry [1], namely: bilateral, rotational, translational, and glide-reflectional. Of these, the bilateral symmetry is dominant over all other types of symmetries [1,2]. Since Symmetry attracts the psychological attention of humans as well as computers [3], it plays an important role in the description and recognition of various objects as well as the understanding of scenes in computer vision and specially robotics [1]. Symmetry has thus an important role in various applications like face analysis [4], indexing of image databases [5], segmentation and detection [6,7], shape completion [8], detection of vehicles [9], and medical image analysis.

The contribution of this paper is a simple method for detecting bilateral symmetry within medical and real world images by simply comparing the gradient magnitude and orientation of the key points. The key points are obtained by extracting SIFT based features from the input image. The success of the method is primarily dependent on the efficiency of the feature detector, i.e. SIFT. Hence, if SIFT extracts fewer than the required features, in the candidate symmetry area, then the detection rate may be low and the results may suffer. The more the SIFT detect the features, more reliable would be the result. Hence the method requires only robust centroid point of the object. If the detected centroid point conforms the true one, then our approach detects symmetry as ground truth. This validation is done by the manual inspection of the ensued results.

The rest of the paper is structured as follows. Section briefly outlines the related work. The details of our approach are given in

Section. The results of our method, when applied to real world images, are elaborated in Section 0.4. Section 0.6 concludes the paper.

## Related Work

The detection of Symmetry has a long history, dating back to 1970's [10] and since then it had got considerable attention of the researchers, in general [11–15]. Mancas, Gosselin and Macq [16] detect tumors in medical images, using the bilateral symmetry, by drawing a vertical line called 'M' located at the middle of the image. They compute the symmetry simply by subtracting the histogram of the two halves. If the resultant is close to zero, then the two halves are declared symmetric and vice versa. The method is, however, restricted to human body only. Li, Zhang and Kleeman [6] propose a technique to detect bilateral symmetry using the edge pixels for real time applications, like robotic vision. First they convert the image to edge image using Canny's edge detector and then on the basis of edge pixels they detect the line of symmetry. In [7], they extend their own idea to compare the gradient of edge pixels and also detect symmetry in skewed objects. But both the given approaches do not encounter the entire image halves.

Lowe [17] extracts the SIFT feature points and then detect the similarities of the same object in two different images by matching the descriptor vectors of the stored key points with the sensed data. Loy and Eklundh [18] detect bilateral symmetry from features' constellation, by extracting SIFT [17] features to handle bilateral symmetric objects with strong background clutter. Once extracted, each feature has a descriptor vector of 128 elements. They only calculate the mirror descriptor vector for each original one, and then match the original with mirror i.e. cross matching. If the original is match with the mirror and vice versa, then the pair will

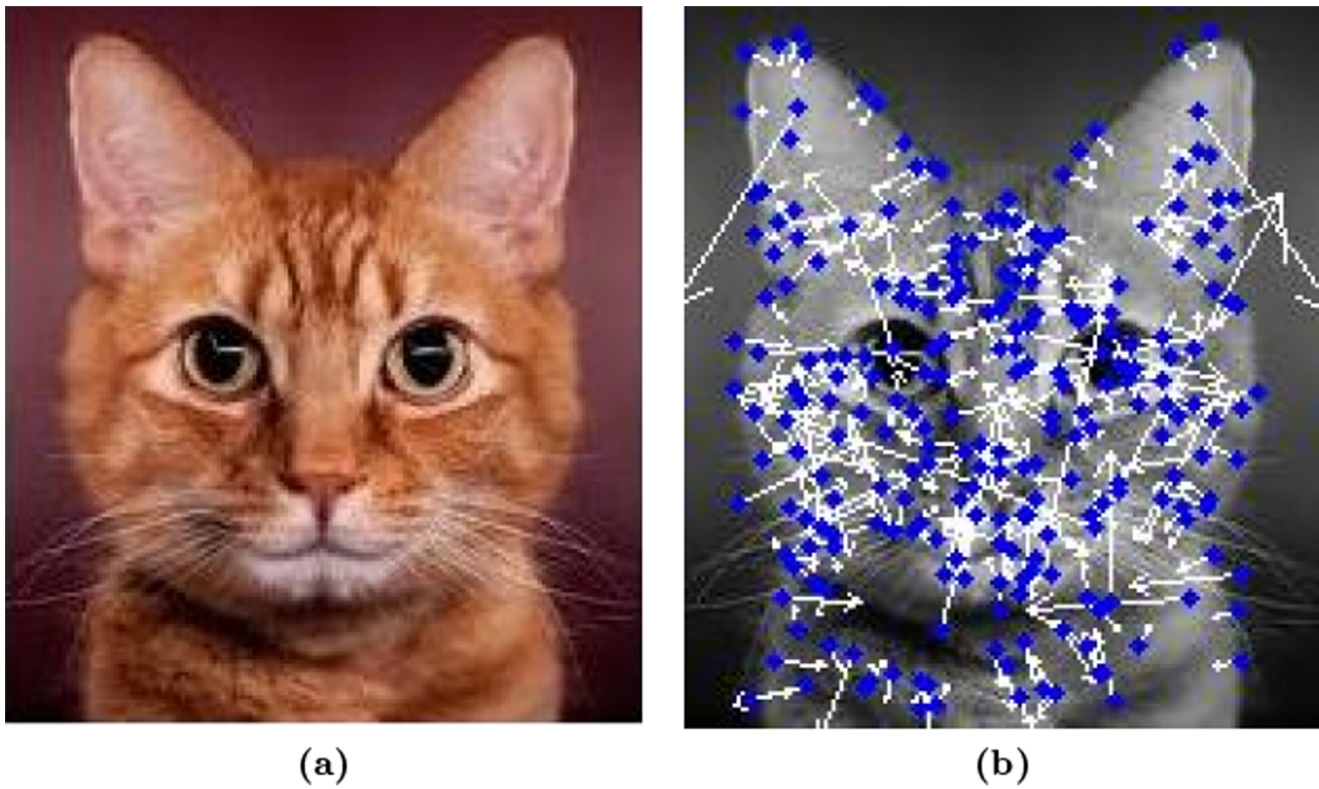


**Figure 1. Convert to intensity image and extract the feature points Using SIFT.** (a) Original image, (b) After treatment.  
doi:10.1371/journal.pone.0103561.g001

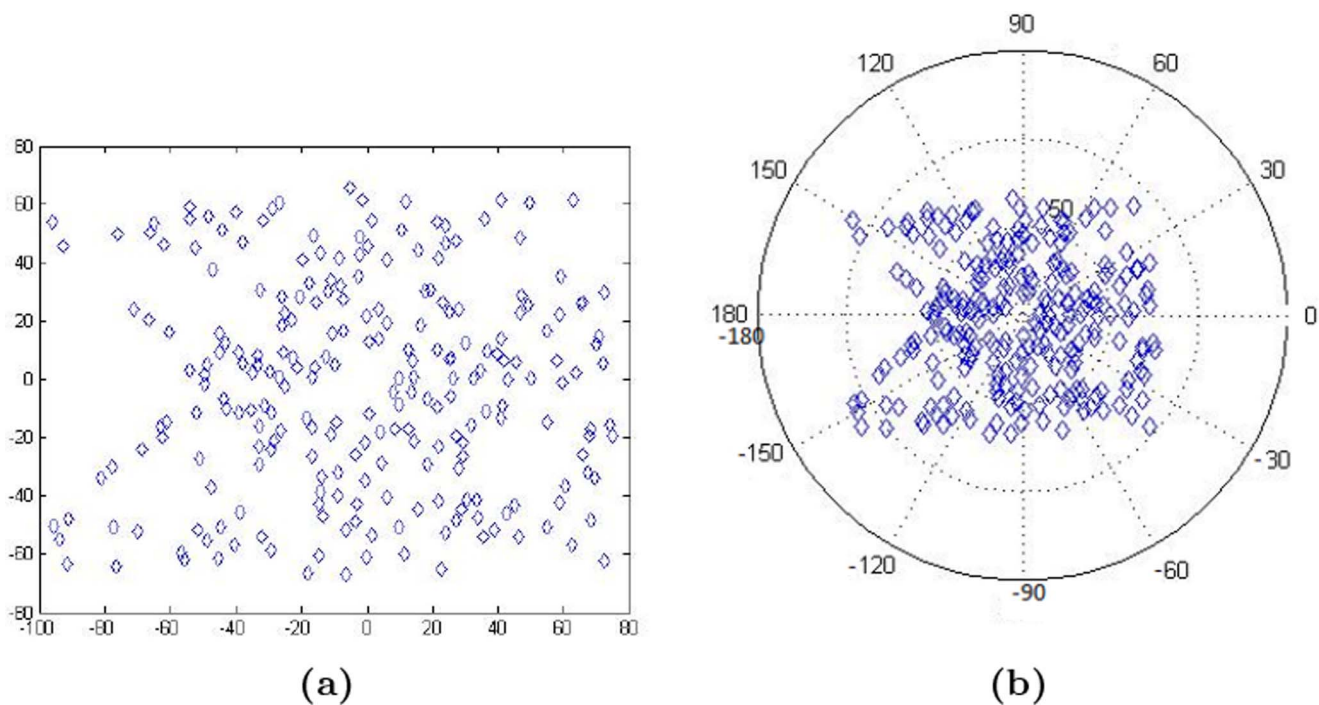


**Figure 2. The coordinate systems.** (a) Cartesian, (b) Polar.  
doi:10.1371/journal.pone.0103561.g002

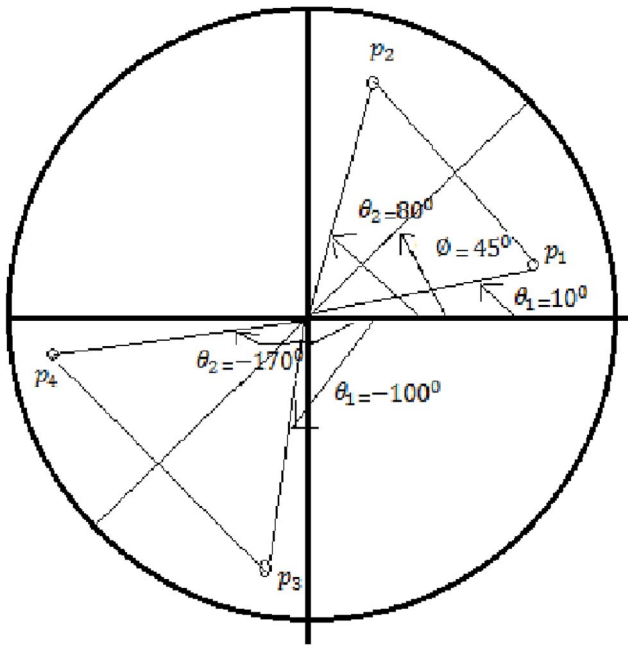


**Figure 3. Calculating symmetric points.**  
doi:10.1371/journal.pone.0103561.g003

be symmetric otherwise not. Once symmetric pairs extracted, then on the basis of symmetry magnitude for each pair, they draw a line of symmetry. Liu and Liu [19] extend the idea of [18] in order to detect the curved reflectional symmetry. They first find the symmetric pair points and their middle point, then establish a pairwise consistency graph among all symmetric pair practical's by applying some thresholds values. The line of symmetry is obtained by calculating the Normalize Cross Correlation(NCC) score among the gradients of the original patches in the trapezoid. If the NCC score is above the threshold value, say 0.5, then an edge is imposed among the particles otherwise not. Lee and Liu [20]

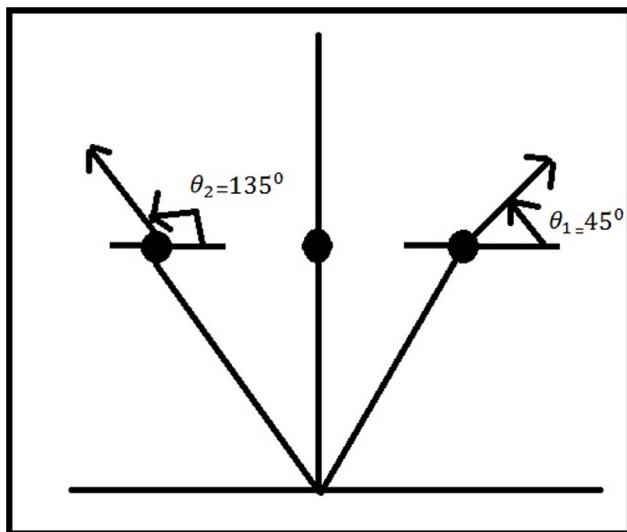


**Figure 4. Comparing gradient magnitude and orientation.**  
doi:10.1371/journal.pone.0103561.g004



**Figure 5. Line of symmetry joining midpoints.**  
doi:10.1371/journal.pone.0103561.g005

extend the idea of [18] and detect the curved and curved glide reflectional symmetry. They add the translation component to the reflection. If the translation is zero then the symmetry will be curved reflectional otherwise it will be curved glide reflectional. They extract symmetric pairs and the direction of symmetry line from the orientations of points i.e. pairwise symmetry. The symmetry line is drawn by using the RANdom SAMple Consensus (RANSAC) algorithm in order to fit a curve in 3D Access Parameter Space(APs).

## The Proposed Method

### 0.1 Overview

Our approach is based on the feature points extraction through the SIFT algorithm [21] that extract features, which are invariant with respect to scale, affine transformation (rotation/translation etc.), illumination, 3D view point and noise [17]. On the basis of these feature points, we compute the centroid of the object and draw those in the Cartesian  $x, y$  coordinate system. It is followed by the conversion to the polar coordinate system, in order to facilitate the extraction of symmetric point pairs. In the end the gradient magnitude and orientation of the corresponding symmetric pair points are compared to evaluate the symmetry among the point pairs.

### 0.2 The procedure

For a given candidate line of symmetry, our approach detects symmetry as follows.

1. First some preprocessing is applied to the input image, if required. This may include RGB to intensity image conversion, noise removal and contrast enhancement etc.
2. The resultant intensity image is subjected to SIFT algorithm in order to extract feature points.
3. Ascertain the centroid point of the object of interest by computing the median point of features points, and then subtract the median from all other points in order to find the centroid point. The centroid point is thereby mapped on the origin of the  $x, y$  coordinate system.
4. Convert to polar coordinate system in order to extract symmetric point pairs by applying the basic mathematics rules. In polar coordinate system, each point is represented by  $r$  and  $\theta$ , where  $r$  is the distance of the point from the origin and  $\theta$  is the angle made with the polar axis. Two points,  $(r_1, \theta_1)$  and  $(r_2, \theta_2)$ , are symmetric with respect to polar axis if  $r_1 = r_2$  and  $|\theta_1| = |\theta_2|$ . We impose two thresholds,  $T_r$  and  $T_\theta$ , on the differences of  $r$ -part and  $\theta$ -part of corresponding point pairs, respectively, in order to ascertain their symmetry with respect

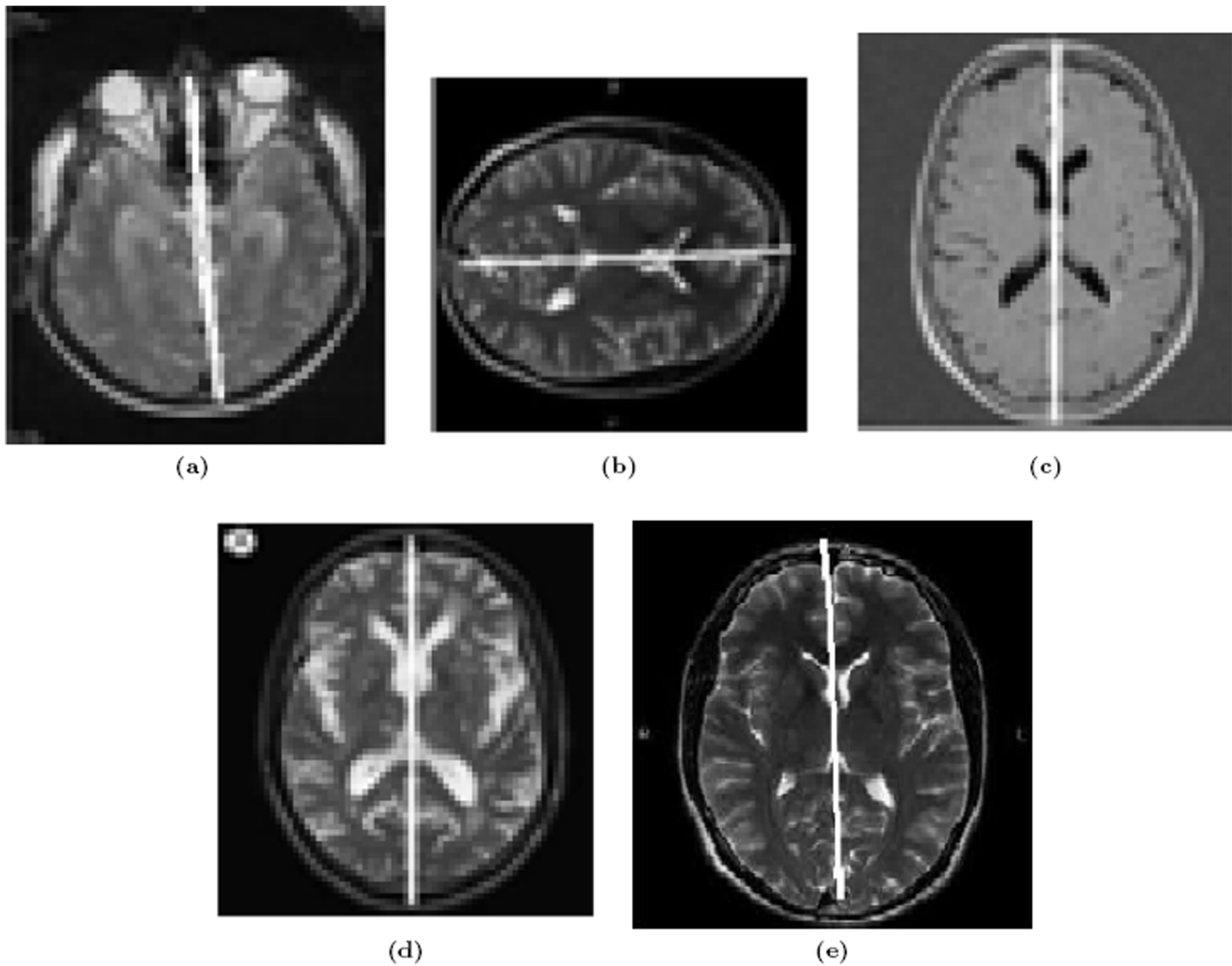


**Figure 6. True Positive Results for medical images.** (a)–(e) are various examples.  
doi:10.1371/journal.pone.0103561.g006

to the polar axis. If both the thresholds are respected, then the points will be symmetric otherwise not.

$$|r_1 - r_2| \leq T_r$$

**AND**

$$(\theta_1 - \phi) - (\theta_2 - \phi) + 360^\circ \leq T_\theta,$$

if  $\theta_1 < 0$  and  $\theta_2 < 0$ ,

$$(\theta_1 - \phi) + (\theta_2 - \phi) \leq T_\theta,$$

elsewhere.

Where  $r_1, r_2$  are distances of the key points from the origin and  $\theta_1, \theta_2$  are the respective angles they make with the polar axis, and  $\delta_\theta$  is the degree of increment in order to rotate the line.

5. Once the symmetric point pairs are extracted, the next task is to evaluate the amount of symmetry exhibited by each pair. This is carried out by comparing the gradient magnitude and orientation of the corresponding point pairs with respect to the candidate line of symmetry. The gradient magnitude and orientation are computed via difference pixels from a fixed  $N \times N$  window around each key point, and then convolve the gradient magnitude with a  $2D$  Gaussian function in order to get a weighted magnitude. The gradient magnitude and orientation are accumulated into a histogram - having, say 36 bins each with a period of 10. The orientation is then assigned to each key point based on the gradient magnitude, i.e. if the gradient magnitude is greater than, say 80%, then the corresponding degree will be assigned to that point.

We set two thresholds, namely  $T_M$  (between 5 and  $-5$ ) and  $T_O$  (between 2 and  $-2$ ), on the gradient magnitude and gradient orientation, respectively and if both thresholds are satisfied according to the following criteria then the points, in a given pair, will be declared symmetric, otherwise not:



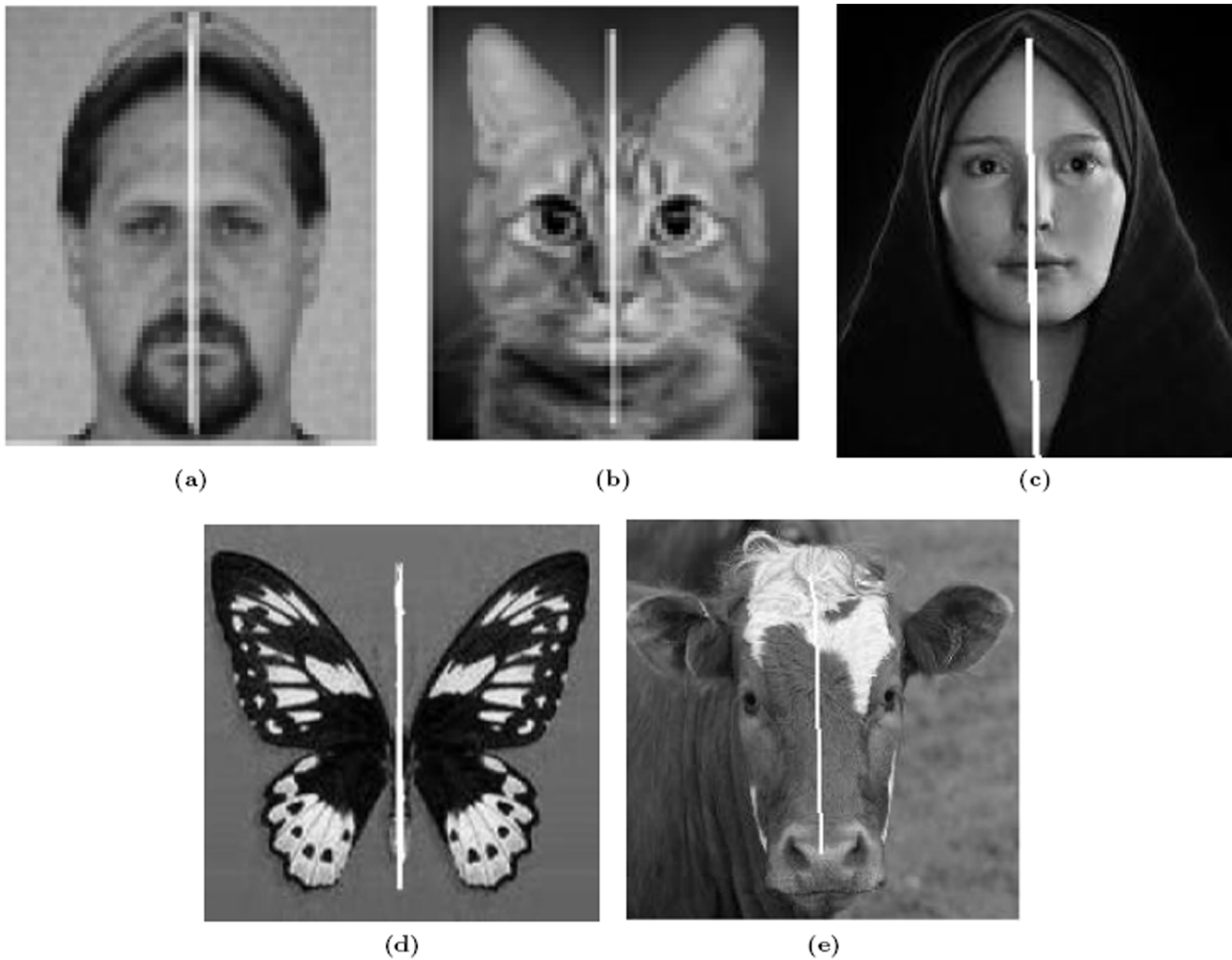


**Figure 7. True Positive Results for real-world images.** (a)–(e) are various examples.  
doi:10.1371/journal.pone.0103561.g007

$$|M_i - M_j| \leq T_M$$

$$|Q(i) + Q(j) - 2\phi| \leq T_Q,$$

**AND**

$$|(Q(i) + Q(j) - 2\phi) + 360^\circ| \leq T_Q,$$

if  $Q(i) < 0$  and  $Q(j) < 0$ ,

elsewhere.

Where  $\mathbf{M}$  is the gradient magnitude and  $\mathbf{Q}$  is the gradient orientation of the key points.

- For each point pair, compute the midpoint of the line joining the two points and draw the line joining all such midpoints.

Our approach selects the final line of symmetry among  $m$  lines, the one which has greater number of symmetric point pairs, i.e.

**Table 1.** The confusion matrix for experimental dataset.

Test outcome	True Positives	False Negatives
Symmetric	94.47%	5.53%
Asymmetric	0%	100%
	False Positives	True Negatives

doi:10.1371/journal.pone.0103561.t001

**Table 2.** Comparison of our Approach with Loy's Method.

Test outcome	Our Approach	Loy
Images without background clutter	95.47%	95.47%
Images with background clutter	60.5%	90.9%

doi:10.1371/journal.pone.0103561.t002

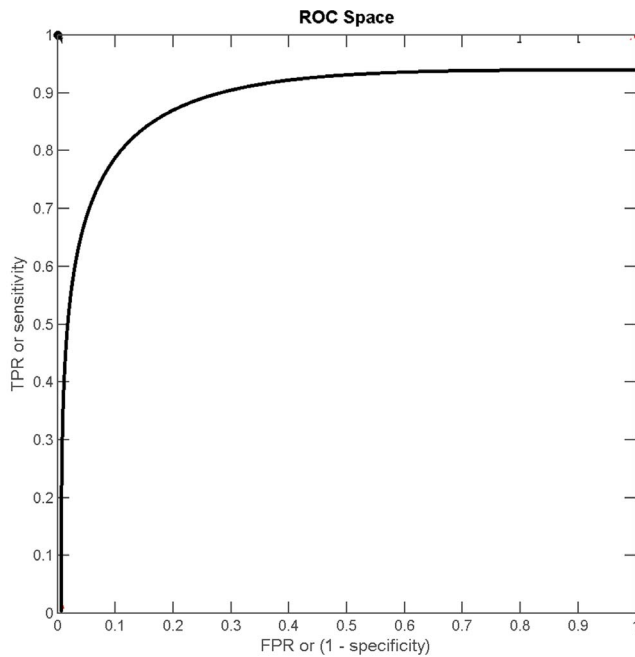


**Figure 8. The receiver operating characteristic response.**  
doi:10.1371/journal.pone.0103561.g008

the line against which more symmetric pairs points are detected by our approach. Each pair polls a single vote for symmetry line. A pair will be symmetric if steps 4 and 5 are true, otherwise not.

### 0.3 The candidate lines of symmetry

Our method starts checking the symmetry against the polar axis, i.e. assuming the latter to be the line of symmetry and applying the above procedure to ascertain the symmetry. The candidate line of symmetry is then rotated at fixed increments,  $\delta_\theta$ , and at each increment the above procedure is repeated. The procedure is stopped when the total increment in rotation reaches 180 degrees. At the end the list of those lines are maintained against which the symmetry has been ascertained by the above procedure. This procedure allows us to check exactly  $m$  ( $= 180/\delta_\theta$ ) candidate lines for symmetry. A given candidate line makes an angle  $\phi$  with the polar axis resulted after  $k$  increments, i.e.  $k \times \delta_\theta = \phi$ , where  $0 \leq \phi < 180^\circ$ .

### 0.4 Statistical measures

In order to summarize the experimental results, we are relying based on the confusion matrix. In the confusion matrix, *true positive* means the symmetry reported by our approach in symmetric object, *false negative* means asymmetry reported by our approach in objects which were actually symmetric. *False positives* mean those asymmetric objects which were wrongly identified by the algorithm as symmetric, while *true negatives* imply asymmetric objects correctly classified as asymmetric.

To identify positive results, *sensitivity* is calculated as under.

$$\text{sensitivity} = \frac{\# \text{ of True Positives}}{\# \text{ of True Positives} + \# \text{ of False Negatives}} \quad (1)$$

For identifying negative results, *specificity* is calculated with the following formula.

$$\text{specificity} = \frac{\# \text{ of True Negatives}}{\# \text{ of True Negatives} + \# \text{ of False Positives}} \quad (2)$$

## Results

### 0.5 Example illustration

As an illustration we are demonstrating the results of our method when applied to the example image, given in Figure 1a. The original image was converted to its intensity image, before subjecting it to SIFT. Then passed the intensity image to SIFT feature extractor to extract feature points, as shown in Figure 1b.

The next step is to compute the centroid point of the object based on the extracted features. A representation of the points drawn in  $x, y$  coordinate system is shown in Figure 2a. The centroid point is invariant to image rotation with SIFT. Things become easier if one converts to the polar coordinate system in order to extract symmetric pairs points. This may be attributed to the fact that, in polar coordinate system, the rotation of the line is easier to comprehend. In addition, the symmetric pairs are readily identifiable from the feature constellation via the simple symmetry rules in the polar coordinate system, as shown in Figure 2b.

Rather than having the range of  $0^\circ$  to  $360^\circ$ , the implementation takes  $0^\circ$  to  $180^\circ$  counter clockwise, i.e. positive, and  $-1^\circ$  to  $-180^\circ$  clockwise. For our purpose, we have imposed two small thresholds,  $T_r$  and  $T_\theta$  on the distance and angle difference, respectively.

Our first candidate line of symmetry is the polar axis, i.e.  $\phi = 0$ , followed by the lines at successive angle increments of  $\delta_\theta$ ; a total of  $180/\delta_\theta$  candidates. Against each line, we return point pairs whose  $r$ -difference and  $\theta$ -difference respect the  $T_r$  and  $T_\theta$  thresholds, respectively. For example, if after  $k$  successive increments, the candidate line is at angle ( $\phi$ ) of 45 degrees to the polar axis, our algorithm calculate the symmetric pairs against this line as follows as shown in Figure 3.

Let  $P_1(7, 10^\circ)$  and  $P_2(7, 80^\circ)$  be two points, then angles of both the points are positive, so  $(\theta_1 - \phi) + (\theta_2 - \phi) \leq T_\theta$  is true, i.e.

$$7 - 7 = 0 < T_r$$

and

$$(80 - 45) - (10 - 45) = 0 < T_\theta$$

Both the thresholds are respected, so the points are symmetric.

Similarly if  $P_3(8, -100^\circ)$  and  $P_4(8, -170^\circ)$  be two points, then angles of both the points are negative, so  $(\theta_1 - \phi) - (\theta_2 - \phi) + 360 \leq T_\theta$  is true, i.e.

$$8 - 8 = 0 < T_r$$

and

$$(-100 - 45) - (-170 - 45) + 360 = 0 < T_\theta$$

**Table 3.** The confusion matrix for Medical and real World Images.

Test outcome	True Positives	False Negatives
Real World Images	95.47%	4.53%
Medical Images	85.1%	14.9%

doi:10.1371/journal.pone.0103561.t003

Once symmetric pairs are extracted, then we compare the gradient magnitude and orientation of the corresponding points in each pair. The symmetry of gradient information's is ascertained by comparing with the values of  $T_M$  and  $T_Q$  as shown in Figure 4.

Let  $\theta_1$  and  $\theta_2$  are gradient orientations of two key points, both angles are positive, then  $|Q(i) + Q(j) - 2\phi| \leq T_Q$  is true, and

$$(45 + 135 - 2 * 90) \leq T_Q$$

The symmetry measure of each pair is quantified as a function of relative location, gradient magnitude and orientation. If any one of the two condition is false, the pair will not be counted as symmetric.

Next midpoints of each point pairs are computed and joined to get the line of symmetry; of all the candidates the one with maximum point pairs is designated as the line of symmetry, as the one shown in Figure 5.

## 0.6 Other Results

The feature points are detected using Lowe's SIFT code [17]. On the basis of these feature points, our approach detects bilateral symmetry within medical and real world images as shown in Figure 6 and Figure 7, respectively. We have tested our algorithm on medical and real-world images with strong boundary condition - i.e. frontal images of bilateral symmetric objects - taken from various sources on the Internet. In total, 1209 single object images were collected, of which 899 were symmetric images and 310 were

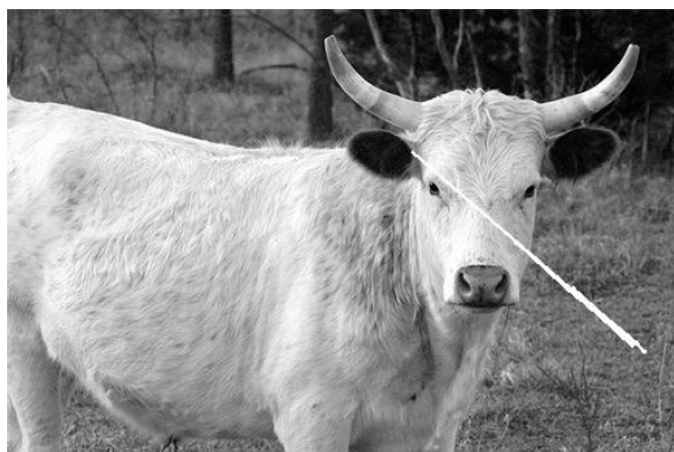
asymmetric. Out of the former, 799 were with no background clutter while 100 were with background clutter. As can be seen in Table 1, our method identified 788 images, out of the 799 symmetric images (with no background clutter), correctly. This amounts to a sensitivity of 94%. In the case of asymmetric images 310 out of 310 were correctly identified. With frontal symmetric objects, the detection rate of our approach is at par with the method by Loy and Eklundh [18]. For images with background clutter, however, our results are inferior, as evident from Table 2.

Figure 8 shows the Receiver Operating Characteristic (ROC) response of our algorithm and its consequential performance, having a curve near to the ideal case. The method has a high area under the curve, being near to 0.92, where the maximum is 1. The detection rate for medical images has been found comparatively low, because in such images the symmetry line is not straight; it is a bit curved. Hence our approach detects the symmetry line approximately nearly to the ground truth line. The detection rates of our approach for medical and real world images are shown in Table 3 in the form of a Confusion Matrix. For real world images, the detection rate has been higher, because most real world objects have a straighter line of symmetry.

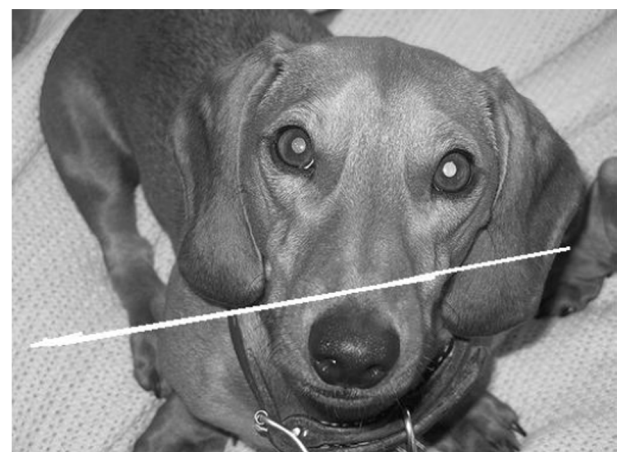
Two of the example images, where the results are not satisfactory, are shown in Figure 9. Though the contained objects are symmetric, wrong centroids are computed due to too many features in the background. It is to be noted over here that our method would correctly classify symmetric objects only when they appear 'symmetric' in the image. In each image of Figure 9, the contained object is by itself symmetric but the way it is photographed, does not give a symmetric view and only the head part constitutes a symmetric object which is unfortunately not detachable from a background that mostly includes the torso. Such kind of 'localized' symmetry cases are against our assumption of single-object image.

## Conclusion

The results have been more than satisfactory, provided that the input image is a single object image. With asymmetric objects, the method classified those correctly each time. With symmetric objects too, the outcomes were enviable and only those objects were misclassified which were either partially captured or



(a)



(b)

**Figure 9. False Negative Results.** (a) and (b) are examples.

doi:10.1371/journal.pone.0103561.g009

occluded, or with something in the background. In future we intend to target multiple objects and multiple lines as well as other three aspects of symmetry. Even within asymmetric objects one can identify symmetric parts after some essential pre-processing.

## References

- Liu Y, Hel-Or H, Kaplan CS, van Gool IJ (2010) Computational symmetry in computer vision and computer graphics. *Foundations and Trends in Computer Graphics and Vision* 5: 1–195.
- Park M, Lee S, Chen PC, Kashyap S, Butt AA, et al. (2008) Performance evaluation of state-of-the-art discrete symmetry detection algorithms. In: *Computer Vision and Pattern Recognition Conference (CVPR'08)*: 1–8.
- Kootstra G, Nederveen A, Boer BD (2008) Paying attention to symmetry. In: *Proc. the British Machine Vision Conference (BMVC'08)*.
- Mitra S, Lazar NA, Liu Y (2007) Understanding the role of facial asymmetry in human face identification. *Statistics and Computing* 17: 57–70.
- Sharvit D, Chan J, Tek H, Kimia BB (1998) Symmetry-based indexing of image databases. In: *Proc. IEEE Workshop on Content-Based Access of Image and Video Libraries*. pp. 56–62. doi: 10.1109/IVL.1998.694496.
- Li WH, Zhang AM, Kleeman L (2006) Real Time Detection and Segmentation of Reflectionally Symmetric Objects in Digital Images. In: *IEEE/RSJ Int. Conf. on Intelligent Robots and Systems*. pp. 4867–4873. doi:10.1109/IROS.2006.282442.
- Li WH, Zhang AM, Kleeman L (2005) Fast global reflectional symmetry detection for robotics grasping and visual tracking. In: *Proceedings of Australasian Conference on Robotics and Automation*.
- Zabrodsky H, Peleg S, Avnir D (1993) Completion of occluded shapes using symmetry. In: *Proc. IEEE Computer Society Conference on Computer Vision and Pattern Recognition (CVPR '93)*. pp. 678–679. doi:10.1109/CVPR.1993.341031.
- Kuehne A (1991) Symmetry-based recognition of vehicle rears. *Pattern recognition letters* 12: 249–258.
- Davis LS (1977) Understanding shape: II. Symmetry. *IEEE Trans on Systems Man and Cybernetics (SMC'1977)* 7(3): 204212.
- Marola G (1989) On the detection of the axes of symmetry of symmetric and almost symmetric planar images. *IEEE Trans Pattern Analysis and Machine Intelligence* 11: 104–108.
- Masuda T, Yamamoto K, Yamada H (August 1993) Detection of partial symmetry using correlation with rotated-rected images. *Pattern Recognition* 26(8): 1245–1253.
- Reisfeld D, Wolfson H, Yeshurun Y (1995) Context free attentional operators: the generalized symmetry transforms. *Int. Journal of Computer Vision* 14(2): 119–130.
- Loy G, Zelinsky A (2003) Fast radial symmetry for detecting points of interest. *IEEE Trans Pattern Analysis and Machine Intelligence* 25: 959–973.
- Keller Y, Shkolnisky Y (2004) An algebraic approach to symmetry detection. In: *Proc. 17th Int. Conf. on Pattern Recognition (ICPR'04)*. volume 3, pp. 186–189. doi:10.1109/ICPR.2004.1334499.
- Mancas M, Gosselin B, Macq B (2005) Fast and Automatic Tumoral Area Localisation using Symmetry. In: *Proc. IEEE Int. Conf. on Acoustics, Speech, and Signal Processing (ICASSP'05)*. volume 2, pp. 725–728. doi:10.1109/ICASSP.2005.1415507.
- Lowe DG (2004) Distinctive image features from scale invariants key point. *International journal of computer vision*.
- Loy G, Eklundh JO (2006) Detecting Symmetry and Symmetric Constellations of Features. In: *Proc. 9th European Conference on Computer Vision - Volume Part II*. Berlin, Heidelberg: Springer-Verlag, ECCV' 06, pp.508–521. Available: [http://dx.doi.org/10.1007/11744047\\_39](http://dx.doi.org/10.1007/11744047_39).
- Liu J, Liu Y (2010) Curved reection symmetry detection with self validation. *Computer Vision-ACCV'10*: 102–114.
- Lee S, Liu Y (2012) Curved Glide-Reection Symmetry Detection. *IEEE Trans Pattern Analysis and Machine Intelligence* 34: 266–278.
- Lowe DG (1999) Object Recognition from Local Scale-Invariant Features. In: *Proc. Int. Conf. on Computer Vision*. Washington, DC, USA: IEEE Computer Society, volume 2 of *ICCV '99*, pp. 1150–. Available: <http://dl.acm.org/citation.cfm?id=850924.851523>.

## Author Contributions

Conceived and designed the experiments: HA KH NH. Performed the experiments: HA. Analyzed the data: KH NH UIB. Contributed reagents/materials/analysis tools: KH. Wrote the paper: HA KH.